DIAMOND–LIKE CARBON FILMS DEPOSITED BY A TRIODE PECVD UNDER TWO LEVELS OF ACETYLENE FLOW RATE

Oliveira, P.E.
Fundação Centro Tecnológico de Minas Gerais (CETEC)
Av. José Cândido da Silveira 2000, Cidade Nova, Belo Horizonte, MG, 31170–000
paulo.oliveira@cetec.br

Borba, E.C.
Fundação Centro Tecnológico de Minas Gerais (CETEC)
Av. José Cândido da Silveira 2000, Cidade Nova, Belo Horizonte, MG, 31170–000
elenice.borba@cetec.br

Muniz, E.P.
Fundação Centro Tecnológico de Minas Gerais (CETEC)
Av. José Cândido da Silveira 2000, Cidade Nova, Belo Horizonte, MG, 31170–000
eduardo.muniz@cetec.br

Gomes, S.H.F
Fundação Centro Tecnológico de Minas Gerais (CETEC)
Av. José Cândido da Silveira 2000, Cidade Nova, Belo Horizonte, MG, 31170–000
sammuca_1999@yahoo.com.br

Vilela, J.M.
Fundação Centro Tecnológico de Minas Gerais (CETEC)
Av. José Cândido da Silveira 2000, Cidade Nova, Belo Horizonte, MG, 31170–000
jose.mario.vilela@cetec.br

Moura, C.W
Departamento de Engenharia Mecanica, FCTUC, Universidade de Coimbra
Pinhal de Marrocos, 3030, Coimbra, Portugal
carlos.moura@dem.uc.pt

Ramanery, F.P.
Fundação Centro Tecnológico de Minas Gerais (CETEC)
Av. José Cândido da Silveira 2000, Cidade Nova, Belo Horizonte, MG, 31170–000
fabio.ramanery@cetec.br

Saturnino, D.M.
Fundação Centro Tecnológico de Minas Gerais (CETEC)
Av. José Cândido da Silveira 2000, Cidade Nova, Belo Horizonte, MG, 31170–000
dsaturnino@bol.com.br

Branco, J.R.T.
Fundação Centro Tecnológico de Minas Gerais (CETEC)
Av. José Cândido da Silveira 2000, Cidade Nova, Belo Horizonte, MG, 31170–000
jose.branco@cetec.br

Abstract. *We studied the tribological behavior of diamond–like carbon (DLC) films produced from acetylene in a plasma enhanced chemical vapor deposition (PECVD) system. Films were deposited on AISI 304 stainless steel samples prepared by the deposition of different amounts of acetylene. Measurements of ball–cratering (Calotest) and scratching resistance were done to evaluate the wear resistance and the adhesion of the films. FTIR, AFM and RAMAN spectroscopy technics were used to elucidate the structural chemistry of each film and correlate it to the tribological properties.*

Keywords*: DLC, PECVD, deposition conditions, tribology*

1. Introduction

The hard layers of amorphous hydrogenated carbon (a–C:H) generated by Plasma Enhanced Chemical Vapor Deposition (PECVD) are being largely studied because of their wide applicability in mechanic resistance, biomedicine and semiconductor materials. Its potential high hardness, sometimes above 20 GPa, with low friction coefficient can result in high abrasion resistance (Robertson, 1999). The deposition technique, PECVD, has a large industrial application, because of the possibilities of uniform coating of large areas at temperatures near ambient. Grill (1999) stated that the most important limiting factors are the low adhesion to some metallic substrates, which is caused by the lack of occurrence of stable interfaces, in opposition of films deposited over Si substrates, in which a thin SiC layer is formed and the high residual inner tension which limits the maximum useful layer thickness.

In the last decade, a great background has been obtained about the structure of DLC films deposited by PECVD and their relationship with the following deposition parameters: total deposition gas pressure and substrate bias tension (Grill, 1999). These two factors together set the most important structural characteristic of a–C:H films, the sp^3/sp^2 bond ratio of the carbon atoms (Robertson, 2002), which determines the optical, electrical and tribological properties (Silva *et al*, 1998).

In an effort to give more PVD systems higher flexibility to hybrid processing, the paper investigates the feasibility of a triode ion plating system to deposit DLC films. The effect of two different acetylene flows for the deposition of DLC over substrates previously nitrated at temperatures of 300°C is evaluated.

2. Experimental procedures

The films studied in this paper were obtained by deposition of acetylene in a chamber with a total volume of 640 l, at temperatures of 300°C, pressure of 2.3×10^{-3}mbar. The samples were previously nitrated by a 90 sccm nitrogen flow and the process gas (acetylene) was supplied to the deposition chamber according to conditions described in Tab. 1. A plasma torch was formed by a argon source operated at 720W. The samples were heated and etched by the plasma for 15 min. before the coating and held in a rotary apparatus in 3 positions (Fig. 1), being placed in the distances showed in the Tab. 2.

Table 1. Deposition conditions

Condition	Acetylene flow (sccm)	Deposition time (min)
I	40	30
II	80	60

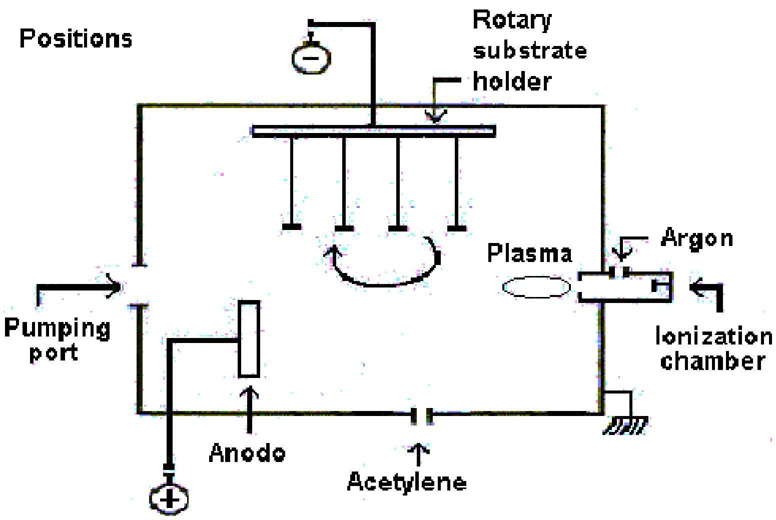

Figure 1. Schematic diagram of deposition chamber

Table 2. Vertical distances from the plasma for sample positions (cm)

Position	Dist. from the plasma (cm)
A	22
B	14
C	6

Reflection – absorption infrared (FTIR) measurements were made with a BOMEN DA8 machine, 500 scans were done for each spectrum and the resolution was 4 cm^{-1}. Raman spectra were measured in the Metallurgical Engineering

Dept. of UFMG using a JOBIN YVON HORIBA equipment, model LABRAN 800 with visible laser excitation (λ = 632 nm) with a 2 cm^{-1} precision in the value of the measured Raman shift. Atomic Force Microscopy (AFM) fom Digital Instruments, model Dimension 3000, operating on tapping mode, was used to verify the topography three–dimensional of thin films. The surface scanning of the films was done with a commercial silicon probe.

The ball–cratering (Calotest) tests were carried out using a ball–cratering tribometer developed by the Laboratory of Engineering and Surface Modifications (LEMS) of CETEC, and shown in Fig. 2. The apparatus consists of a bearing steel ball rotating against a metallic wear plate with abrasive paste (diamond paste, medium diameter of 1 μm) passing between the contact points. The steel ball is a standard 41.3 mm bearing ball and it is rotated by means of an engine fitted with a spin–counter device. The scratching resistance tests were done in a CSAM REVETEST equipment, with a loading between 0 and 20 N, with a vertical velocity of 60 N.min^{-1} and a horizontal velocity of 30 mm.min^{-1}. Two scratches were done in each sample.

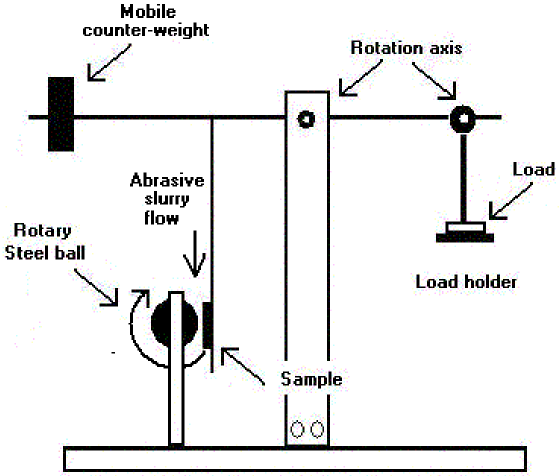

Figure 2. Schematic diagram of the ball–cratering tribometer

3. Results and Discussion

Table 3 shows the areas under the curve (I) of the absorption bands associated with sp^3 and sp^2 structures in DLC films deposited at different distances from the plasma for condition II (acetylene ratio of 80 sccm, deposition time of 60 min.).

Table 3. Areas of the absorption bands due to stretching modes of sp^3 and sp^2 structures for DLC deposited at different distances from the plasma (condition II)

Position	Dist. Plasma (cm)	I_{sp3} (cm^{-1})	I_{sp2} (cm^{-1})
A	22	69.3	4.0
B	14	79.3	5.3
C	6	52.8	2.1

The FTIR spectra of the samples show a CH_n stretching band which can be divided in two areas, one from 2800 up to 2960 cm^{-1}, created by the absorption modes of CH_2 and CH_3 stretching in sp^3 (diamond like) configurations (Demichelis, 1995; Giorgis, 1997; Prado, 1997; Robertson, 1999; Robertson, 2002; Saw, Idrus e Ibrahim, 2000; Zhang et al., 1998) and the other, from 2960 up to 3085 cm^{-1} (Robertson, 1999; Giorgis, 1997), due to the stretching of these compounds in sp^2 configurations.

It is known that, while essentially all sp^3 sites in a–C are hydrogenated, many sp^2 sites are not (Robertson, 1999). So, it is not possible to use the relation between the area of the absorption band in the FTIR due to sp^3 C–H stretching modes and the area of the band due to sp^2 C–H stretching modes to get an exact value of the relation between the amount of sp^2 and sp^3 carbon atoms in the sample. But, by the same argument, the area of the sp^2 C–H stretching band can be used as a way to measure the minimum value of sp^2. Logically, we can't compare the area of the sp^2 band directly with the area of the sp^3 one since they have different absorption strengths associated with them. But, if normalization is done to eliminate the effect of different thickness (or different optical paths) it is logical to compare the area of the sp^3 band in one sample with the area in another the same being valid for the sp^2 one.

From Tab. 3 it is possible to see that the sp^3 (diamond) content is larger for a distance of 14 cm from the plasma, with a final reduction for little distances.

Raman spectroscopy gives important details about bonding structures of DLC films. The C–C diamond bonds show a well defined Raman active mode around 1332 cm^{-1}, whereas single crystal graphite (C=C vibration mode on the hexagonal chain plane) has a single Raman active mode at 1580 cm^{-1} labelled "G" (for 'graphite'). At 1350 cm^{-1} appears the disordered graphite second mode (named "D" for 'disordered') (Robertson, 2002).

The Raman spectra of DLC films deposited under condition I (acetylene ratio of 40 sccm, deposition time of 30 min.) at distances of 22 and 6 cm from the plasma are compared in Fig. 3.

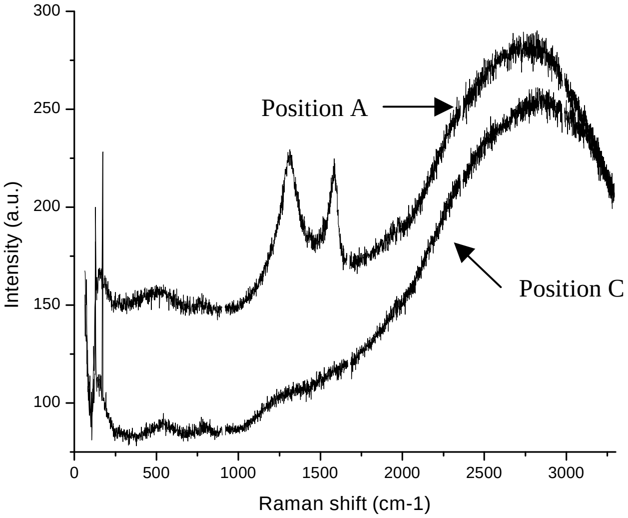

Figure 3. Raman spectra of deposited films at different distances from the plasma for condition I (acetylene ratio of 40 sccm, deposition time of 30 min.)

We observe the occurrence of an active mode in 1327 cm^{-1}, a graphite active mode at 1599 cm^{-1} and great hump modes centered around 2750 and 2850 cm^{-1} respectively. According to Robertson (2002), the G and D modes dominates the Raman spectra of a–C by scattering of the sp^2 sites. The π states are lower energy than the σ states and so they are much more polarisable, giving to the sp^2 sites 50–230 times larger Raman cross–section than sp^3 sites. The observed modes, on the other hand, show a strong peak on 1327 cm^{-1} which could be attributed to the left shifted 'disordered' graphite peak. It is possible to note that a great proximity with the plasma is harmful to the sp^3 and sp^2 structures formation, probably because of the shortage of ionized gas on the plasma sheath.

Table 4 shows the wear rate measured by the ball–cratering tests for samples by conditions I and II. According to these data, we found a larger wear rate for the DLC sample at condition I in position B than at condition II at the same position. For the condition I, a position near the plasma caused a gain of wear resistance of near ten times. Table 4 shows as well that for condition II, there is no difference between the obtained data for the both positions.

Table 4. Wear rate measured by the ball–cratering tests for samples obtained by conditions I and II.

Condition	Position	Wear rate (m^2/N)
I	B	$2.2\text{x}10^{-14}$
	C	$1.0\text{x}10^{-15}$
II	B	$1.1\text{x}10^{-15}$
	C	$1.1\text{x}10^{-15}$

The final (or exiting) scratch damages caused in samples deposited in position B at both conditions are shown in Fig. 4. The horizontal and vertical double–sided arrows indicate that, while in condition I a scratch larger than that in condition II was done, condition II presented a major loss of adhesion, as can be seen due to the great film lifting at the exiting extremity of the indenter tip. We conclude that a smaller deposition of acetylene (by smaller flux and time) causes, therefore, a scratch resistance loss, on the other hand, it is easier to cause damage to a film deposited by a larger amount of the deposition gas. Supplementary tests are being done to evaluate film thickness and confirm the above findings.

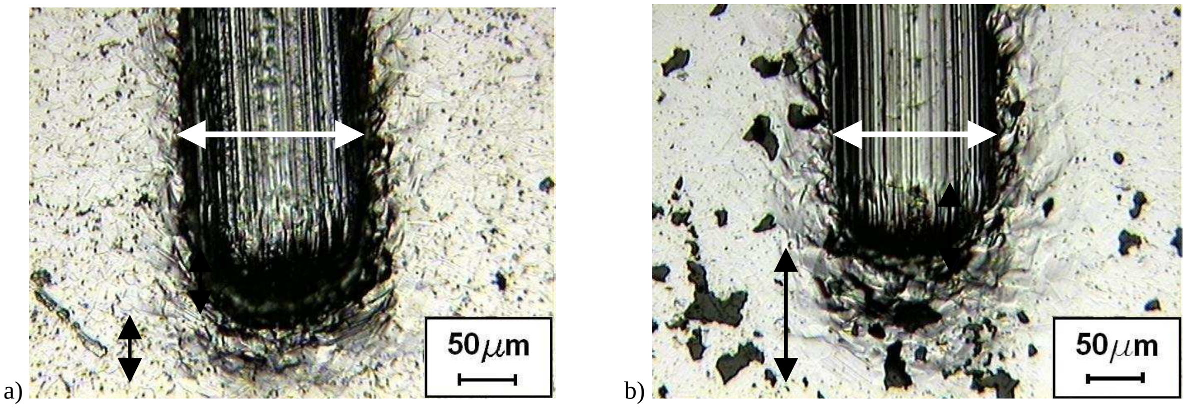

Figure 4. Optical image of scratch damage to samples at a) condition I and b) condition II (both samples in position B)

Figure 5 compares the AFM topological analysis of samples obtained under both conditions and position B, by three-dimensional images of 2 µm sided square areas.

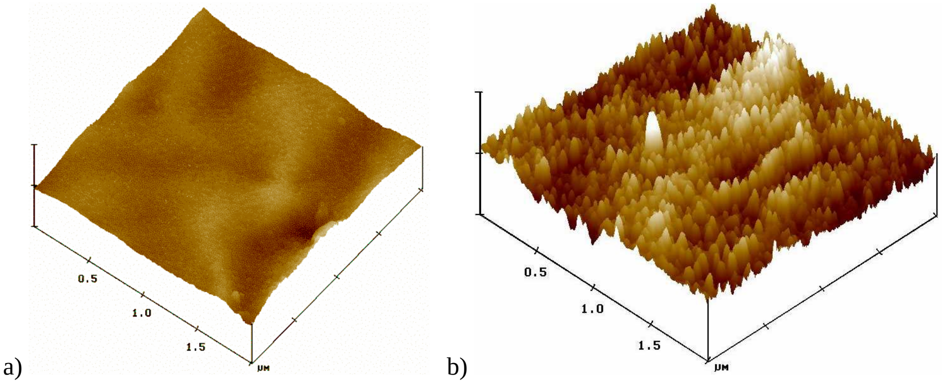

Figure 5. AFM three-dimensional images of samples at a) condition I and b) condition II (both samples in position B)

Is possible to see more acute spikes on the sample obtained by condition II, suggesting that this phenomenon was caused by acetylene molecules in excess. The roughness evaluated by AFM techniques is 3.661 nm for condition I and 3.278 nm for condition II, in spite of the film features mentioned above. The lower roughness for the higher acetylene content of condition II indicates higher film uniformity and perhaps less substrate influence. The subsequent thickness evaluation is being done to support this analysis.

4. Conclusions

In this study, DLC deposited by a new triode ion plating processing has been evaluated. It was verified that sp^3 content varies with the acetylene flow rate, which affected the wear rate and surface roughness.

5. Acknowledgements

This project was supported by CEMIG / ANEEL. The authors are thankful to Maria Silvia Silva Dantas (Metalurgical Engineering Dept. of UFMG) for the Raman measurements, to Leandro Gomes Silva and Elaine Reis for the scratching resistance measurements and to Tatiana Renata Gomes Simões for the IR measurements.

6. References

Robertson, J., 1999, "Hard amorphous (diamond–like) carbons", Progress in Solid State Chemistry, Vol. 21.

Grill, A., 1999, "Diamond–like carbon: State of the Art", Diamond and Related Materials, Vol. 8, pp.428–434.

Robertson J., 2002, "Diamond–like amorphous carbons Materials Science and Engineering", R 37, pp.129–281.

Silva, S. R. P., Robertson, J., Milne, W. I., Amaratunga, G. A. J. (eds.), 1998, "Amorphous carbon: state of the art", World Scientific, Singapore.

Freire Jr., F. L., 1995, "Amorphous hydrogenated carbon nitride films obtained by plasma–enhanced chemical vapor deposition", Japanese Surface and Coating technology, Vol.74–75, pp.382–386.

Liu Y. and Cohen, M., 1989, "Prediction of new low compressibility solids", Science, Vol. 245, pp.841–842.

Franceschini, D. F., Achete, C. A. and Freire Jr., F. L., 1992, "Internal Stress Reduction by Nitrogen Incorporation in Hard Amorphous Carbon Films", Applied Physics Letters, Vol. 60, pp.3229–3231.

Prado, R.J., 1997, "Propriedades Químicas e Morfologicas de Filmes Hidrogenados de Carbeto de Silício Amorfo", Instituto de Física, Universidade de São Paulo: São Paulo, 123 p. (Tese de doutorado).

Saw, K.G., R.M. Idrus, and K. Ibrahim, 2000, "Diamond–like amorphous carbon thin films by d.c. magnetron sputtering". Journal of Materials Science Letters, Vol. 19, p.735–737.

Zhang, Q., et al., 1998, "Deposition of hydrogenated diamond–like carbon films under the impact of energetic hydrocarbon ions". Journal of Applied Physics, Vol. 84, No. 10, pp.5538–5542.

Demichelis, F. et al., 1995, "Structural and optoelectronic properties of carbon–rich hydrogenated amorphous silicon–carbon films". Diamond and Related Materials, Vol. 4, No. 4, p.357–360.

Giorgis, F. et al., 1997, "a–SiC:H films deposited by PECVD from silane + acetylene and silane + acetylene + hydrogen gas mixture". Diamond and Related Materials, Vol. 6, p.1606–1611.

5. Responsibility notice

The authors are the only responsible for the printed material included in this paper.